Electronic Properties, Band Structure, and Fermi Surface Instabilities of Ni^{1+}/Ni^{2+} Nickelate $La_3Ni_2O_6$, Isoelectronic with Superconducting Cuprates

Viktor V. Poltavets and Martha Greenblatt

Department of Chemistry and Chemical Biology, Rutgers University, 610 Taylor Road, Piscataway, New Jersey 08854, USA

Gerhard H. Fecher and Claudia Felser

Institute for Inorganic and Analytical Chemistry, Johannes Gutenberg University, 55099 Mainz, Germany

(Received 6 March 2008; published 28 January 2009)

Electronic structure calculations were performed for the mixed-valent Ni^{1+}/Ni^{2+} nickelate $La_3Ni_2O_6$, which exhibits electronic instabilities of the Fermi surface similar to that of the isostructural superconducting $La_2CaCu_2O_6$ cuprate. $La_3Ni_2O_6$ shows activated hopping, which fits to Mott's variable-range-hopping model with localized states near the Fermi level. However, a simple local spin density approximation calculation leads to a metallic ground state. The calculations including local density approximation + Hubbard U and hybrid functionals indicate a multiply degenerate magnetic ground state. For electron-doped $La_2ZrNi_2O_6$, which is isoelectronic with $La_2CaCu_2O_6$, an antiferromagnetic insulating ground state is found when correlations are included. The nickelates are thus ideal model systems for a deeper understanding of correlated transition metal compounds, magnetism, and superconductivity.

DOI: 10.1103/PhysRevLett.102.046405 PACS numbers: 71.20.Ps, 71.18.+y

Currently, there is much excitement about the high temperature superconductors based on FeAs layers [1]. Competition between magnetism and superconductivity is considered in these materials [2]. The FeAs intermetallic compounds and the classical cuprate high temperature superconductors have similar low-dimensional (LD) crystal structures [3], are at the border line to magnetism [2], and show spin density wave (SDW) instabilities [4]. It was the observation of the SDW state in $BaFe_2As_2$ [5] that guided Johrendt's group to search for superconductivity in the doped compound [6]. Superconductivity in the FeAs systems occurs in the doped compounds or can be induced by suppressing the magnetism by applying high pressure [7]. Nickel-containing compounds such as $LuNi_2B_2C$ are structurally related to $BaFe_2As_2$ [2] and become superconducting at higher temperatures (16 K) [8]. The fact that LD structure types are favorable for superconductivity inspired us to look for possible candidates for superconductivity in nickelates, which are isoelectronic with the cuprates.

Bednorz and Muller started their exploration for superconductivity in the La-Ni-O system with Ni in oxidation states 3 + /2+ [9]. Their discovery of high-T_c superconductivity in cuprates [10] motivated an extensive search for similar phenomena in nickelates. It was shown, however, by local density approximation (LDA) calculations including Coulomb correlations (LDA + U) that most of the mixed-valent nickelate phases are considerably different from the superconducting cuprates [11]. The oxides with a Ni^{3+} formal oxidation state do not form magnetic insulators but localized $S = 1$, Ni^{2+} states embedded in a sea of itinerant O holes [11]. Only if the Ni^{1+} ions are forced into a planar coordination with the O ions is a $S = 1/2$ magnetic insulator realized that possibly can be doped with low spin ($S = 0$) Ni^{2+} holes in analogy with the high-T_c cuprates [11].

Ni^{1+} nickelates are not often investigated due to their chemical instability [12]. The Ni^{1+} ion in $LaNiO_2$ has a $3d^9$ electronic configuration as Cu^{2+} in the isostructural $CaCuO_2$. $LaNiO_2$ is, however, reported to be nonmagnetic and probably metallic, whereas $CaCuO_2$ is a magnetic insulator [13]. In $LaNiO_2$, additional La-$5d_{xy}$ states leave a band with Ni $3d$ character pinned to the Fermi level [13]. The recently discovered mixed-valent Ni^{1+}/Ni^{2+} nickelate $La_3Ni_2O_6$ [12] shares with the superconductive Cu^{2+}/Cu^{3+} cuprates a common structural element—the infinite MO_2 (M = Ni, Cu) planes and identical electronic configuration. Thus, this particular nickelate may be a direct analog of the superconducting cuprate $La_2CaCu_2O_6$ that is an antiferromagnetic (AFM) insulator and becomes superconducting at 60 K by hole doping [14]. The present work reports transport properties together with the results of electronic structure calculations of pure and electron-doped $La_3Ni_2O_6$ in comparison to La_2CaCu_2O6. To account for the electronic correlations, the calculations were performed beyond the local density approximation by LDA + U and hybrid functionals.

$La_3Ni_2O_6$, as well as all known nickelates with infinite NiO_2 square-planar layers, are members of the T'-type $Ln_{n+1}Ni_nO_{2n+2}$ (Ln = La, Nd; n = 2, 3, and ∞) homologous series [12,15]. The structures of the T'-type nickelates can be described as built by stacking of alternating ($Ln/O_2/Ln$) fluorite-type layers with $Ln_{n-1}(NiO_2)_n$ infinite layer structural blocks [12] (Fig. 1). The so-called double ($n = 2$) and triple ($n = 3$) layer T'-type nickelates are unique examples of such structural arrangements. Although the structure of $La_2CaCu_2O_6$ is formed by alternating perovskite and rocksalt blocks, this double-layered

Ruddlesden-Popper cuprate is structurally the closest analog among cuprates to $La_3Ni_2O_6$ nickelate (Fig. 1). Both phases crystallize in the $I4/mmm$ (no. 139) space group. The $(Ln/O_2/Ln)$ fluorite-type layers in $La_3Ni_2O_6$ can serve as a charge reservoir similar to the LaO rocksalt layers in $La_2CaCu_2O_6$. The most important difference in the crystal structures is the coordination of the $3d$ elements, i.e., square-pyramidal coordination of Cu and a square-planar environment of Ni.

The electronic structure was calculated by the full potential linearized augmented plane wave method as implemented in WIEN2K [16]. The exchange-correlations functional was taken within the generalized gradient approximation (GGA) [17]. LDA is not able to describe the magnetic state of such highly correlated systems properly [18]. The LDA + U approach allows the most important on-site correlations [19,20]; LDA + U was successfully applied to describe various electronic properties of cuprates; see, e.g., Ref. [21]. To account for on-site correlation, the LDA + U method with U from 1 to 10 eV was used in the self-interaction correction scheme with $J = 0$. In particular, the value of $U = 7$ eV comes close to the one usually used for the Mott insulator NiO. Similar values were used in the calculations of $LaNiO_2$ [13] and La_2NiO_4 [11]. Another approach to describe the oxides correctly is the use of exact exchange in Hartree-Fock (HF) -based hybrid functionals [22–24]. Here, the B3PW (a three-parameter combination of the Becke exchange functional [25] with the PW-GGA [26] and the HF scheme) hybrid functionals were selected [27]. To allow for an AFM setup of the spins at different atoms, the crystal structure reported in Ref. [12] was transformed from $I4/mmm$ (space group no. 139) to $I4mm$ (no. 107) symmetry.

The calculated band structures are shown in Fig. 2. Independent of the magnetic order, steep bands are crossing the Fermi energy in the ΓN, ΓP, and XP directions, indicating that the compound is metallic. Along the ΓX direction, where the bands have a flat dispersion just above or below ϵ_F, they exhibit van Hove singularities of the saddle point type. In the antiferromagnetic case, two highly dispersive bands are nearly degenerate, and such band "doubling" is a result of the bilayered character of the crystal structure. These bands comprise states derived from the Ni-$d_{x^2-y^2}$ and in-plane oxygen O-$2p_x$ and p_y states. The origin of the high dispersion within the layers (Γ-X-Z) is due to the d_{x^2}-$_{y^2}$ orbitals of Ni ions pointing directly toward the four oxygen neighbors within the layers. Hopping of electrons between neighboring Ni ions is thus possible through the chessboardlike ordering of the $3d$ metal ions. The bands show no dispersion along Z-Γ, which is perpendicular to the planes. For $La_3Ni_2O_6$ two saddle points, one 0.12 eV above and the second 0.14 eV below ϵ_F are found along X and Γ. The nickelates La_2 MNi_2O_6 (M = Zr, Hf) are isoelectronic with the cuprates and show a similar Fermi surface nesting as $La_2CaCu_2O_6$ (compare [28]). This nesting may render possible spin density wave instabilities. Such a nesting instability is found in superconducting cuprates and FeAs compounds [4] and shows that electron-electron correlations have to be taken into account.

To investigate the magnetic properties, spin-polarized calculations were performed assuming an AFM ordering of the nickelate similar to that found in $La_2CaCu_2O_6$ as well as ferromagnetic (FM) ordering. Different from the results of Lee and Pickett for $LaNiO_2$ [13], the AFM and the FM ground states of $La_3Ni_2O_6$ are nearly degenerate. The energy difference between the FM and the AFM ground states is small (about 0.2 meV). Similar to $LaNiO_2$, a magnetic moment of $0.53\mu_B$ is found on the Ni ions. The total moment per formula unit is $1.089\mu_B$. Overall, the spin-polarized calculations of $La_3Ni_2O_6$ were very unstable with respect to final convergence, independent of the method used. Such problems were not observed in the spin-polarized calculations for $La_2CaCu_2O_6$. This suggests that the instabilities arise from the degenerate magnetic ground state of $La_3Ni_2O_6$ with nearly equal total energies

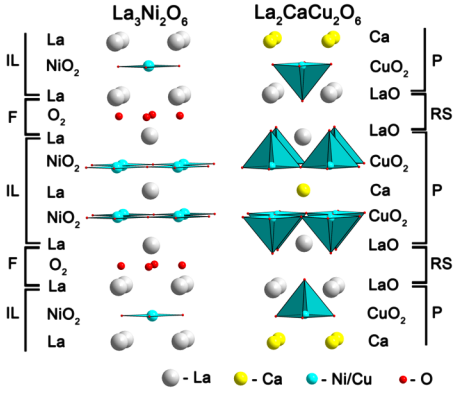

FIG. 1 (color online). Crystal structures of $La_3Ni_2O_6$ and $La_2CaCu_2O_6$ with denoted layers and structural blocks: P, perovskite; RS, rocksalt; IL, infinite layer; F, fluorite.

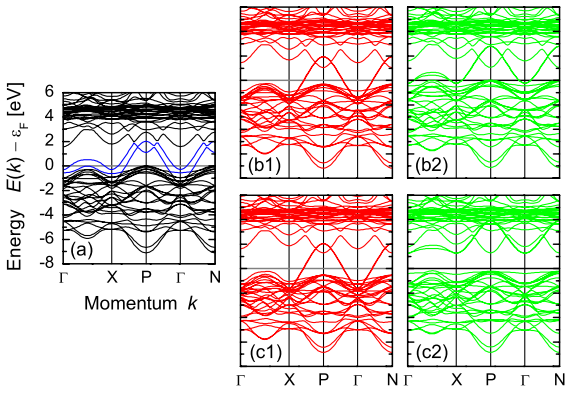

FIG. 2 (color online). The band structure of $La_3Ni_2O_6$. (a) shows the GGA calculation for the antiferromagnetic state. The corresponding ferromagnetic majority and minority bands are shown in (b1) and (b2), respectively. The LDA + U calculation results in a half-metallic ferromagnetic state [majority (c1), minority (c2)].

of the FM and AFM states independent of the calculational scheme.

To estimate the influence of electron-electron correlations, the FM and AFM states were calculated in the LDA + U scheme and compared to the B3PW exact exchange method with the Hartree-Fock scheme for the exchange part of the hybrid energy functional. Remarkably, already a small Hubbard U of about 1.4 eV transfers the metallic FM state into a half-metallic FM state with a gap of about 0.55 eV in the minority states [compare Fig. 2(b) with Fig. 2(c)]. The size of this gap increases with U and is about 1.5 eV for $U \approx 3.5$ eV or when using hybrid functionals. Concerning the magnetic properties, the results from LDA + U with $U \approx 3.5$ eV and from the B3PW hybrid functional agree very well. Comparing the total energies of the FM and AFM states, no pronounced differences are recognized, independent of the calculational method (including $U = 0$). The FM and AFM ground states are obviously also degenerate, when correlations are included.

To make the importance of the electron-electron correlation more clear, the density of states calculated for the AFM state by different methods is shown in Fig. 3. The non-spin-polarized density from GGA is shown for comparison and makes clear that such an approach is unrealistic for correlated systems. However, it is also seen that this density differs not much from the spin-averaged AFM calculation. It is clear by comparing the spin-polarized AFM densities [Fig. 3(b)] and Figs. 3(c) and 3(d) how the states are shifted away from the Fermi energy under the influence of an increasing correlation. The same shift is observed for the hybrid functional [Fig. 3(e)] where the correlations are better accounted for. In particular, the changes observable in the unoccupied states may be more reliable from the hybrid functional approach [22].

For comparison, the electronic structure of $La_2CaCu_2O_6$ was calculated using LDA + U. The electronic structure of the materials is compared in Fig. 4 ($U = 7$ eV). As for the nickelate, the results for this value of U are very similar to those from the hybrid functionals. The Ni compound stays metallic [Fig. 4(a)], whereas the Cu compound becomes semiconducting [Fig. 4(c)], when electron correlations are included. The size of the indirect gap amounts to about 300 meV, whereas the optical gap at Γ is much larger (2.2 eV). A similar opening of the gap was reported for $LaCuO_3$ and La_2CuO_4 [29]. The magnetic moments at the two Cu atoms with antiparallel spins are about $\pm 0.8 \mu_B$. As mentioned above, even LDA + U is unable to split the steep band crossing ϵ_F in $La_3Ni_2O_6$. It stays pinned to the lowest completely unoccupied band. In contrast, this band is shifted by correlations completely below ϵ_F in $La_2CaCu_2O_6$. As a result, all valence bands are shifted away from ϵ_F. This is the reason why it seems that U has a stronger effect on the cuprate than on the nickelate. Obviously, the differences between the two compounds are due to the different numbers of valence electrons in the primitive cell, 65 in $La_3Ni_2O_6$ and 66 in $La_2CaCu_2O_6$. To have a nickelate with the same electron count as the cuprate, one may replace one La by an element of group IVB, for example, Zr or Hf. The calculations reveal that both $La_2ZrNi_2O_6$ and $La_2HfNi_2O_6$ exhibit a gap at ϵ_F in the band structure and thus become semiconducting if electron correlations are respected. The calculated magnetic moments at the two Ni atoms are $\pm 1.5 \mu_B$ and $\pm 1.4 \mu_B$ in the AFM state.

We have performed transport measurements on polycrystalline pressed pellets of $La_3Ni_2O_6$ in the temperature range of 5–400 K with a standard four-probe technique. The fit of the resistivity (ρ) data to Mott's variable-range-hopping model (Fig. 5) with localized states near the Fermi level [30]

$$\rho = \rho_0 \exp(T_0/T)^{\alpha} \qquad (\alpha = 1/4) \tag{1}$$

yields $\rho = 4\ \mathrm{k\Omega\,cm}$ at 300 K, $T_0 = 3.1 \times 10^7$ K, and $\rho_0 = 8 \times 10^{-5}\ \Omega$ cm. The observed degree of localization as manifested by the magnitude of T_0 is large. The discrepancy among the LDA + U, metallic, and observed semiconducting behavior is attributed to the measurement made on a polycrystalline pressed pellet of the sample. For the layered structure of $La_3Ni_2O_6$ (Fig. 1), highly anisotropic transport properties are expected: metallic conduc-

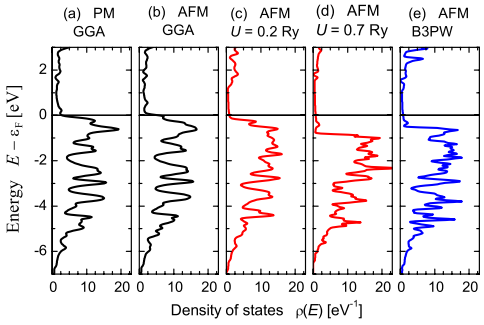

FIG. 3 (color online). Comparison of the density of states of $La_3Ni_2O_6$ for different functionals.

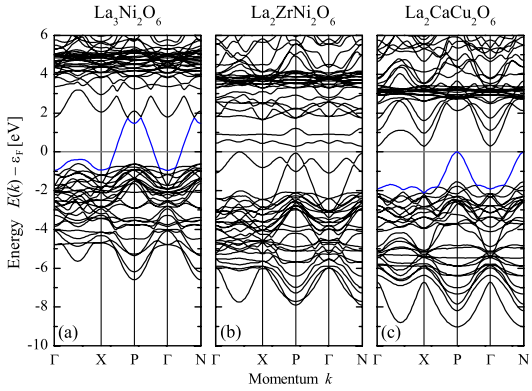

FIG. 4 (color online). Band structure of (a) $La_3Ni_2O_6$, (b) $La_2ZrNi_2O_6$, and (c) $La_2CaCu_2O_6$, calculated for AFM spin orientation at Ni using LDA + U, with $U = 7$ eV.

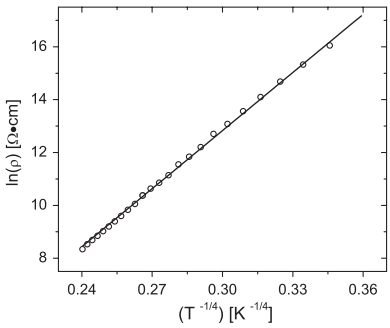

FIG. 5. The natural logarithm of resistivity $\ln(\rho)$ versus $T^{(-1/4)}$ of $La_3Ni_2O_6$; observed data (circles) and fitting curve (solid line) according to Mott's variable-range-hopping model with $\alpha = 1/4$.

tivity in the infinite plane of $Ni^{1+/2+}$-O, while semiconducting or insulating behavior perpendicular to these planes. Evidently, in the polycrystalline sample, the semiconducting property dominates (Fig. 5). Single crystal measurements are required to resolve this discrepancy, but single crystals are difficult or impossible to obtain.

Preliminary magnetic measurements indicate no magnetic order down to 4 K; weak FM is observed in the magnetization versus field (M vs H) at 5 K, which persists at least up to 400 K. This result is consistent with the band structure calculations, which show degenerate FM and AFM ground states. However, we cannot exclude local FM clustering or small Ni metal impurities. No saturation of M is evidenced even at the maximum field of 5 T available in our SQUID.

A fundamentally interesting scenario would be to change the electronic structure of the nickelate by bringing the saddle point (high density of states) and the Fermi energy to coincidence, which might be accomplished in two ways. Substitution of Zr for La or oxygen deficiency should raise ϵ_F to higher energy in the vicinity of the saddle point. Similar chemical doping leads to superconductivity in the cuprate. However, substitution in the nickelate is a challenge, and a FM ground state should compete with superconductivity. The investigation of the transport properties under high pressure may be a better way to lower the saddle point to cross ϵ_F and to suppress FM. Under pressure, the AFM ground state is preferred. Therefore, it may be possible to suppress FM interactions in $La_3Ni_2O_6$ by pressure to induce superconductivity.

In summary, it has been shown that electronic structure calculations of the mixed-valent $La_3Ni_2O_6$ including correlations result in instabilities close to the Fermi energy similar to that of the superconducting cuprate $La_2CaCu_2O_6$. It is concluded that $La_3Ni_2O_6$ is an ideal model system for a deeper understanding of the interplay between magnetism and superconductivity in correlated electronic oxides.

This work was supported by the National Science Foundation through DMR-0233697 and DMR-0541911 at Rutgers and by the German Science Foundation DFG-FE633/4 and the TRR 49 at Johannes Gutenberg University.

[1] Y. Kamihara *et al.*, J. Am. Chem. Soc. **128**, 10 012 (2006).
[2] Y. Kohama *et al.*, Phys. Rev. B **78**, 020512(R) (2008).
[3] L. M. Volkova, Supercond. Sci. Technol. **21**, 095019 (2008).
[4] I. I. Mazin, D. J. Singh, M. D. Johannes, and M. H. Du, Phys. Rev. Lett. **101**, 057003 (2008).
[5] M. Rotter *et al.*, Phys. Rev. B **78**, 020503(R) (2008).
[6] M. Rotter, M. Tegel, and D. Johrendt, Phys. Rev. Lett. **101**, 107006 (2008).
[7] A. Kreyssig *et al.*, Phys. Rev. B **78**, 184517 (2008).
[8] T. Siegrist *et al.*, Nature (London) **367**, 254 (1994).
[9] J. G. Bednorz and K. A. Muller, The Nobel Prize Lecture, http://nobelprize.org, 1987.
[10] J. G. Bednorz and K. A. Muller, Z. Phys. B **64**, 189 (1986).
[11] V. I. Anisimov, D. Bukhvalov, and T. M. Rice, Phys. Rev. B **59**, 7901 (1999).
[12] V. V. Poltavets, K. A. Lokshin, T. Egami, and M. Greenblatt, J. Am. Chem. Soc. **128**, 9050 (2006).
[13] K.-W. Lee and W. E. Pickett, Phys. Rev. B **70**, 165109 (2004).
[14] R. J. Cava *et al.*, Nature (London) **345**, 602 (1990).
[15] V. V. Poltavets *et al.*, Inorg. Chem. **46**, 10 887 (2007).
[16] P. Blaha, K. Schwarz, G. K. H. Madsen, D. Kvasnicka, and J. Luitz, *WIEN2K, An Augmented Plane Wave + Local Orbitals Program for Calculating Crystal Properties* (Karlheinz Schwarz, Technische Universität Wien, Wien, Austria, 2001).
[17] J. P. Perdew, K. Burke, and M. Ernzerhof, Phys. Rev. Lett. **77**, 3865 (1996).
[18] W. E. Pickett, Rev. Mod. Phys. **61**, 433 (1989).
[19] V. I. Anisimov, J. Zaanen, and O. K. Andersen, Phys. Rev. B **44**, 943 (1991).
[20] A. I. Liechtenstein, V. I. Anisimov, and J. Zaanen, Phys. Rev. B **52**, R5467 (1995).
[21] A. N. Yaresko, A. Y. Perlov, R. Hayn, and H. Rosner, Phys. Rev. B **65**, 115111 (2002).
[22] J. Muscat, A. Wander, and N. M. Harrison, Chem. Phys. Lett. **342**, 397 (2001).
[23] J. K. Perry, J. Tahir-Kheli, and W. A. Goddard, Phys. Rev. B **63**, 144510 (2001).
[24] I. P. R. Moreira, F. Illas, and R. L. Martin, Phys. Rev. B **65**, 155102 (2002).
[25] A. D. Becke, J. Chem. Phys. **98**, 5648 (1993).
[26] J. P. Perdew and Y. Wang, Phys. Rev. B **45**, 13 244 (1992).
[27] F. Tran, P. Blaha, K. Schwarz, and P. Novák, Phys. Rev. B **74**, 155108 (2006).
[28] C. Felser, R. Seshadri, A. Leist, and W. Tremel, J. Mater. Chem. **8**, 787 (1998).
[29] M. T. Czyżyk and G. A. Sawatzky, Phys. Rev. B **49**, 14 211 (1994).
[30] N. F. Mott and E. Davis, *Electronic Processes in Non-crystalline Materials* (Clarendon Press, Oxford, 1979).